
Sensitivity Analysis and Control in an Elastic CAD-Free Framework for Multi-Model Configurations

Bijan Mohammadi

Laboratoire ACSIOM

Département de Mathématiques - CC51

Université de Montpellier II

34095 Montpellier

Bijan.Mohammadi@math.univ-montp2.fr

ABSTRACT. This paper presents the extension of our CAD-Free platform to the simulation and sensitivity analysis for design and control of multi-model configurations. The CAD-Free platform has been enriched by an elastic model. We present the different ingredients of the platform and discuss various coupling and control strategies. The targeted configurations gather some unstable aerodynamical behaviour.

RÉSUMÉ. Nous présentons l'extension de notre approche CAD-Free pour la simulation, conception et contrôle de configurations multi-modèle. La plateforme CAD-Free a été enrichie avec un modèle élastique dynamique. Nous présentons les divers ingrédients de la méthode, ainsi que plusieurs algorithmes de couplage et de contrôle. Les configurations envisagées représentent les comportements aéroélastiques instables rencontrés dans les applications.

KEYWORDS : Flow Control, fluid-structure interaction, Sensitivity Analysis.

MOTS-CLÉS: Contrôle d'écoulement, interaction fluide-structure, Analyse des sensibilités.

1. Introduction

Two and three dimensional flutter problems simulation is a challenging task and is interesting for both industrial and academical aspects. Usually, structure design concerns the structural characteristics of the model, something which is usually performed without taking into account the possible flow unsteadiness. At this step, the design accounts often at best for mean flow loads and tries to avoid resonance phenomena for a few flow eigenmodes corresponding to the lowest structural modes where the eigen-analysis is done for each model separately. On the other hand, aerodynamical shape optimization is usually performed for given structural characteristics after adding geometrical constraints on local thickness for instance to guarantee a realistic final shape from structural point of view. Current efforts concern the realization of this task in a MDO (multi-disciplinary) context for steady configurations. In both cases, it is therefore reasonable for the flow to stay in the validity domain of these optimizations, which means as much as possible steady or close to it. We are therefore interested to control unsteadiness which might appear in a fluid/structure system even in cruise condition. One easy way to perform this task is by perturbing the inflow incidence using a real time flap position perturbation prescribed by a fast gradient based minimization algorithm. The sensitivity evaluation and the minimisation tool have therefore to be enough fast. In that sense, different control laws are obtained using different minimization algorithms and the control is in closed loop as the gradient used to define the descent direction comes from the linearization of the state equations (fluid and structure models) and uses the current state [MOH 99], [OPBM 99], [MOH 99b].

In the past, we showed how to perform sensitivity analysis using automatic differentiation in reverse mode for optimization and control problems. We showed that incomplete sensitivities are efficient for control of unsteadiness where the control is considered as unsteady shape optimization involving large number of control parameters. One particularity of this approach is the CAD-Free parametrization of shapes which avoids CAD manipulations during optimization and only requires an interface with the CAD parametrization at final stage (we recall that the initial correspondance between CAD parametrization and the initial surfacic mesh is known) [MOH 95], [MOH 97], [MOH 99]. Our aim here is to show how to add to the CAD-Free control space an elastic model. In that way, the dynamic optimization system, the fluid and the structure solvers work on the same variables.

Incomplete sensitivities are defined by keeping only geometrical contributions in gradients, if both the unsteady cost function and control parameters are defined on the shape [OPBM 99] and if the cost function has both geometrical and state contributions (like in aerodynamical coefficients for instance). This leads to a sensitivity evaluation and dynamic minimization tool where the fluid and structure states can be replaced by the ones coming from more realistic simulations or based on commercial packages for instance. The idea is that the state equations used for the simulation and for sensitivity analysis can be different. The problem of interest here is therefore different in the sense that the number of control parameters is small (basically one) and the control is not defined over the same region than the cost function.

A major point of interest here is to show that instantaneous control is still efficient for cases where the control and cost function are not defined in the same region (as previously). This dynamic control algorithm enables for simultaneous simulation and control. Indeed, the solution of the adjoint problem will not be required for the definition of the control. To this end, we are particularly interested by the complex variable method. This approach is interesting for cases where only one control parameter (like here) is involved as we can access to the gradient of the cost function with respect to this parameter in real time without any linearization or extra solution for the state equation.

2. Fluid and structure state equations

We are interested by the prediction of flutter problems as well as design of structure leading to a higher flutter speed. We propose here a coupling between two models for the flow and the structure behaviour which show the difficulties we have to face when using commercial codes for the physic of the problem.

2.1. Structural model for the elastic CAD-Free parametrization

For the structure, we consider the following dynamic system based on the CAD-Free surface definition. Our aim again is to have only one geometrical entity during simulation and design and this also when doing MDO configurations. The geometrical definition is therefore again the surface discretization (in 2D segments and in 3D triangles). The definition of normals to the surface is therefore an easy task.

The displacement of the CAD-Free definition of the shape in the normal direction $\delta X^{p+1} = [(x_i^{p+1} - x_i^p) \cdot \vec{n}_i^p]^T$ is described by the following PDE involving first and second order time derivatives as well as second and fourth order elliptic operators. The aim here is to recover by a shell type model the behaviour of different structures after identification of the characteristic constants of the model.

Denotes X^0 the initial shape described by the surfacic (shape) nodes in the fluid mesh:

$$M \frac{\partial^2 X}{\partial t^2} + C \frac{\partial X}{\partial t} - K \Delta(X - X^0) - \mu \Delta^2(X - X^0) = F \quad [1]$$

The first two terms involve pointwise behaviour of the shape and the third and fourth terms link the surfacic nodes together. The parameters M (mass), C (damping), K (stiffness) and μ (shell stiffness) encapsulate the mechanical characteristics of the structure. The presence of second and fourth order surfacic space derivatives enables the model to produce both membrane and shell type behaviours and the parameters K and μ have to be identified to reproduce these behaviour. In this work, we consider only membrane type behaviour ($\mu = 0$). $F = \int_{\partial\Omega} (-p + S \cdot \vec{n} \cdot \vec{\tau})$ models the action of the aerodynamic forces on the structure.

2.2. Fluid models

The simplest model for pressure prediction can be the Newton or the cos-square law where the pressure is given by the following algebraic relation:

$$p = p_{\infty} \cos^2(u_{\infty} \cdot \vec{n}), \quad [2]$$

where p_{∞} is the inflow pressure, u_{∞} the inflow velocity and \vec{n} the local normal to the shape. If we aim to include also viscous effects, a similar relation exists giving the amount of the friction based on wall-function approach:

$$S \cdot \vec{n} \cdot \vec{n} \sim 0, \quad S \cdot \vec{n} \cdot \vec{\tau} = \alpha Re_x^{\beta} + \gamma \frac{\partial p}{\partial x}, \quad [3]$$

where $S = (1/Re)(\nabla u + \nabla u^t - (2/3)\nabla \cdot u I)$ is the Newtonian stress tensor, Re_x is the local Reynolds number based on the distance from the beginning of the viscous region and $\partial p / \partial x (= \nabla p \cdot \vec{\tau})$ is the tangential pressure gradient. The unit tangent is defined as $\vec{\tau} = (\vec{T} / |\vec{T}|)$ with $\vec{T} = u_{\infty} - (u_{\infty} \cdot \vec{n}) \cdot \vec{n}$.

These relations are of course far from being general but their combination is enough to permit the study of various physical behavior we can encounter with more complex models. In addition, this simplicity enables for an evaluation of the CAD-Free elastic parametrization as the state equation is well solved.

The platform also gives the possibility in using more sophisticated fluid models, of course at a higher cost. At this time, NSIKE and NSC(2-3)KE 2 and 3D incompressible and compressible solvers have been interfaced with the elastic CAD-Free parametrization above [NSIKE], [NSC2KE]. We do not describe here these possibilities.

2.3. Fluid-structure interaction

The fluid and structure models presented above enables the evaluation of various coupling algorithms. This subject has been investigated in similar simulations considering two solvers, with an incompatible interface discretization, in parallel requiring informations from each other [DO 92], [CA 96], [NG 94], [SP 95]. With incompatible parametrizations for the fluid and structure interface, a major difficulty comes from information transfert between the two models. As we said, this situation is worse when adding an optimization tool. The following algorithms are therefore valid with any fluid solvers working on the CAD-Free parametrization.

3. Coupling strategies

To present the different strategies possible, we rewrite the second order system (1-2-3) as a first order one:

$$\dot{Z} = f(Z), \quad Z(t = 0) = Z_0, \quad [4]$$

where $Z = \begin{bmatrix} Z_1 \\ Z_2 \end{bmatrix} = \begin{bmatrix} X \\ \dot{X} \end{bmatrix}$ are the new variables and

$$f(Z) = \begin{bmatrix} Z_2 \\ M^{-1}(F(Z_1, Z_2) - C\dot{Z}_2 + K\Delta(Z_1 - Z_1^0)) \end{bmatrix}.$$

In the fluid model above, F does not include Z_2 contribution, but in a more general situation where time derivative is also present in the fluid model, this contribution exists due to an ALE implementation for instance.

3.1. First order explicit coupling

The easiest way to couple two models is a parallel approach, as in the following first order explicit scheme, where both model are advanced in time and the necessary informations are communicated from one model to the other.

$$Z^0 = Z(t = 0), \quad Z^{n+1} = Z^n + \Delta t f(Z^n). \quad [5]$$

3.2. First order implicit coupling

The previous approach has time step limitation, especially due to the stability condition of the structural model. This can be avoided by an implicit version of [5] which leads to:

$$M \frac{Z_2^{n+1} - Z_2^n}{\Delta t} + CZ_2^{n+1} - K\Delta(Z_1^{n+1} - Z_1^0) = F(Z_1^{n+1}). \quad [6]$$

This scheme is also first order accurate.

3.3. First order semi-implicit coupling

The difficulty in the previous algorithm is a too important coupling of the fluid and structure codes. In practice, it is suitable to have an algorithm which requires a separated solution of two codes and if possible no more than one solution of each for each coupling iterations, while algorithm [6] requires a fixed point approach.

3.4. Second order implicit coupling

To improve the accuracy, we use the trapezoidal rule for the integration in time of system [4]:

$$Z_0 = Z(t = 0), \quad Z^{n+1} = Z^n + \Delta t \frac{f(Z^n) + f(Z^{n+1})}{2}, \quad [7]$$

which leads to:

$$M \frac{Z_2^{n+1} - Z_2^n}{\Delta t} + C \frac{Z_2^{n+1} + Z_2^n}{2} - K \Delta \left(\frac{Z_1^{n+1} + Z_1^n}{2} - Z_1^0 \right) = F \left(\frac{Z_1^{n+1} + Z_1^n}{2} \right) \quad [8]$$

where $(Z_1^{n+1} = Z_1^n + \frac{\Delta t}{2}(Z_2^{n+1} + Z_2^n))$.

3.5. Second order coupling with prediction

One difficulty with the implicit schemes [6-8] above is again a too important coupling of the fluid and structure codes. As we said, in practice, it is suitable to advance the two codes separately. This is possible for instance by predicting the structure position needed by the fluid code, and using the predicted fluid state in the structural system:

$$Z_1^{n+1/2} = X^{n+1/2} = 2X^n - X^{n-1} = Z_1^n + Z_2^n \Delta t.$$

The scheme (8) becomes therefore:

$$M \frac{Z_2^{n+1} - Z_2^n}{\Delta t} + C \frac{Z_2^{n+1} + Z_2^n}{2} - K \Delta \left(\frac{Z_1^{n+1} + Z_1^n}{2} - Z_1^0 \right) = F(Z_1^{n+1/2}), \quad [9]$$

which gives (Z_1^{n+1}, Z_2^{n+1}) without recomputing $F(Z)$. This is especially important for complex fluid models.

4. Time dependent minimization problem

We consider the following time dependent minimization formulation for the control of the flutter problem

$$\begin{cases} \min_{\alpha(t)} J(\alpha(t)) = \int_0^T \int_{\partial\Omega(t)} (X(t) - X_{target})^2 d\gamma dt + \int_0^T \alpha(t)^2 dt, \\ E(\alpha(t), X(t), U(t)) = 0, \\ g_1(\alpha(t)) \leq 0. \end{cases} \quad [10]$$

where $\alpha(t)$ denotes the control parameter which is here the inflow angle of attack deviation performed by a flap. $X(t)$ denotes the CAD-Free model deformations and we would like to reach a target position (i.e. avoid flutter for instance). One particularity which has to be introduced is the time lag between the impact of the inflow deviation

on the different points of the shape. To minimize the effort during control, the necessary deviations have to be minimized too and this is the meaning of the second term in the cost function. In this work, we do not take into account this contribution, but rather introduce constraints on the maximum amount of the deviation. This is of course not fully satisfactory. g_1 denotes the constraints on the control parameter (for instance the maximum deviation possible and the maximum realizable frequency by the flap or injection device). We are of course interested by the smallest maximum deviation allowed and the smallest frequency. In addition, we can introduce also geometrical and state (on U) constraints as previously showed on control problem [MOH 99], [OPBM 99], [MOH 99b]. $E(\alpha, X, U)$ denotes the state equations system (1-2-3). As we said, the platform also includes more sophisticated flow and structure solvers [MOH 99], [MOH 99b], [MED 98c], [NSIKE], [NSC2KE], [ME 98d], but their presentation is of no help for the purpose of control algorithm description.

4.1. Second order dynamic system

To solve problem [10], we need an equation for $\alpha(t)$. Consider the following second order time dependent equation for the shape parametrization α .

$$\dot{\alpha} + \epsilon \ddot{\alpha} = -G((\nabla_{\alpha\alpha} J)^{-1}, \nabla_{\alpha} J), \quad [11]$$

where G is a function of the exact or incomplete gradient and of the inverse of the Hessian of the cost function. It also takes into account the projection over the admissible space precised above.

Consider the following discretization in time of [11] (denotes by $\delta\alpha^p$ the control parameter variation at step p):

$$\left(\frac{\epsilon}{\lambda^2} + \frac{1}{\lambda}\right)\delta\alpha^{p+1} = \frac{\epsilon}{\lambda^2}\delta\alpha^p - F((\nabla_{\alpha\alpha}^p J)^{-1}, \nabla_{\alpha^p} J^p).$$

With $\epsilon = 0$, we recover the steepest descent algorithm with fixed step size if the time step λ is fixed and if G does not depend on the Hessian. Of course, λ can be tuned to be optimal at each time step and we recover the optimal steepest descent method which necessarily converges to the closest minimum.

If $\epsilon < 0$, we find the so called heavy ball method [AT 99]. The aim in this approach is to access different minima of the problem and not only the nearest local minimum.

If $\epsilon > 0$, and p -dependent, we recover methods such as conjugate gradient where G has a particular expression. Indeed, the following system without first order time derivative represents the conjugate gradient method:

$$\alpha^{p+1} - 2\alpha^p + \alpha^{p-1} = \Pi(-\lambda^p \|g^p\| \sum_{i=1}^p \frac{g^i}{\|g^i\|} + \lambda^{p-1} \|g^{p-1}\| \sum_{i=1}^{p-1} \frac{g^i}{\|g^i\|}).$$

where $g^i = \nabla_{\alpha}^i J^i$. Note that if λ is fixed and $\|g^p\| = \|g^{p-1}\|$ (like for instance in minimizing a regularized absolute value function), we have

$$\alpha^{p+1} - 2\alpha^p + \alpha^{p-1} = \Pi(-\lambda g^p),$$

which is a discrete second order system without damping meaning that the conjugate gradient method cannot converge if the step size is not optimized.

In the same way, a Newton or quasi-Newton type method can be expressed introducing the inverse of the Hessian or its approximation through a quasi-Newton iterative formula like BFGS for instance where $(\nabla_{xx}^p J)^{-1}$ is approximated by a symmetric definite positive matrix \mathbf{H}^p , constructed iteratively, starting from the identity matrix for instance:

$$\mathbf{H}^{p+1} = \mathbf{H}^p + \left(1 + \frac{\gamma^p{}^T \mathbf{H}^p \gamma^p}{\delta \alpha^p{}^T \gamma^p} \right) \frac{\delta \alpha^p \delta \alpha^p{}^T}{\delta \alpha^p{}^T \gamma^p} - \left(\frac{\delta \alpha^p \gamma^p{}^T \mathbf{H}^p + \mathbf{H}^p \gamma^p \delta \alpha^p{}^T}{\delta \alpha^p \gamma^p} \right), \quad [12]$$

with

$$\gamma^p = \nabla J(\alpha^{p+1}) - \nabla J(\alpha^p).$$

Through this representation, minimization concepts are easy to integrate to a multi-model platform as they consist in adding a new state equation for the parametrization, coupled with the previous existing equations.

4.2. Coupling the control and state equations

Reconsider the system (4), to which we add two new contributions, coming from [11]:

$$\dot{Z} = f(Z), \quad Z(t = 0) = Z_0, \quad [13]$$

where $Z = \begin{bmatrix} Z_1 \\ Z_2 \\ Z_3 \\ Z_4 \end{bmatrix} = \begin{bmatrix} X \\ \dot{X} \\ \alpha \\ \dot{\alpha} \end{bmatrix}$ are the new variables and

$$f(Z) = \begin{bmatrix} Z_2 \\ M^{-1}(F(Z_1, Z_2) - C\dot{Z}_2 + K\Delta(Z_1 - Z_1^0)) \\ Z_4 \\ -\epsilon^{-1}(Z_4 + G(\mathbf{H}(Z_3), \nabla_{Z_3} J)) \end{bmatrix}.$$

We use the semi-implicit algorithm presented above to integrate this system. In particular, we consider the following semi-implicit right-hand-side:

$$f(Z^{n+1/2}) = \begin{bmatrix} Z_2^{n+1} \\ M^{-1}(F(Z_1^{n+1/2}) - C\dot{Z}_2^{n+1} + K\Delta(Z_1^{n+1} - Z_1^0)) \\ Z_4^{n+1} \\ -\epsilon^{-1}(Z_4^{n+1} + G(\mathbf{H}(Z_3^{n+1/2}), \nabla_{Z_3^{n+1/2}} J)) \end{bmatrix},$$

where $Z_1^{n+1/2} = Z_1^n + Z_2^n \Delta t$ and $Z_3^{n+1/2} = Z_3^n + Z_4^n \Delta t$.

The results shown here have been obtained with only first order accuracy for the control part.

5. Sensitivity analysis by CVM

In the past, we widely used automatic differentiation in reverse mode for design and control. In these problems the dynamic minimization equation was seen as an equation for the structure and the control as a time dependent shape optimization problem in CAD-Free framework [MOH 95], [MOH 99]. Therefore, in these configurations the number of control parameters was large. In the problem studied here, the number of control parameter is small. We are interested by the evaluation of the complex variable method for a real time access to the sensitivity of an unsteady cost function (10) with respect to one control parameter (the flap incidence). This method has been widely used by NASA Langley research center group [AN 98], [SQ 98] for sensitivity analysis in aerodynamical problems.

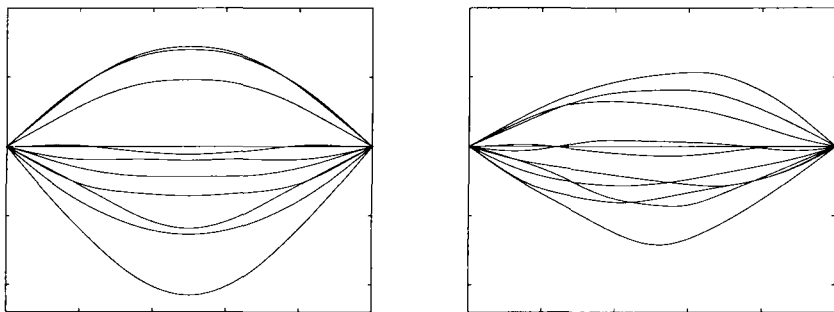


Figure 1. Snapshots of the membrane position without (left) and with (right) control for a vertical inflow impact. Control condition: $h = 10^{-6}$, $\rho = 100$, $f = 100Hz$, maximum deviation $\alpha_{max} = +/ - 10degrees$

A Taylor expansion in the complex plane enables for the definition of the gradient:

$$J(\alpha + i\varepsilon, U(\alpha + i\varepsilon)) = J(\alpha, U(\alpha)) + i\varepsilon J'_\alpha - \frac{\varepsilon^2}{2} J''_\alpha + \varepsilon^2 o(1),$$

therefore

$$\frac{dJ}{d\alpha} = \frac{\text{Im}(J(\alpha + i\varepsilon, U(\alpha + i\varepsilon)))}{\varepsilon} + \varepsilon^2 o(1),$$

We can see that there is no more subtraction and therefore the choice of ε not critical as in finite differences:

$$\frac{dJ}{d\alpha} = \frac{J(\alpha + \varepsilon) - J(\alpha)}{\varepsilon}.$$

In the same way, the second derivative can be found as:

$$\frac{d^2J}{d\alpha^2} = - \frac{Re(J(x_i + i\varepsilon, U(x_i + i\varepsilon))) - J(x, U(x))}{\varepsilon^2}.$$

Unfortunately, here, there is again a subtraction, instead of two when using a central differencing formula ($J''_x = ((J(x + \varepsilon) - 2J(x) + J(x - \varepsilon)))/\varepsilon^2$).

5.0.1. Practical issues

In practice, this methods only requires a redefinition of all real variables of the computer programs in the design loop as complex. This can be seen also as a particular operator overloading approach as in automatic differentiation [OPBM 99]. The complexity of the approach is comparable to first order (forward) finite differences despite the fact that complex operations and storages require twice more effort than for reals but the evaluation of the functional after a small change in the complex plan will not greatly affect the real part:

$$Re(J(x + i\varepsilon)) \sim J(x),$$

therefore only one evaluation is necessary to get J and J' . Of course, the second derivative will not be available anymore. We recover here the same argument as behind incomplete sensitivities. This permits for a real time evaluation of sensitivities for one or few parameters and is interesting for control problems. Of course, the complexity is still proportional to the number of control parameters.

Finite difference method stays however more useful in case where we only have access to black box codes like commercial packages. This is why incomplete sensitivities are really useful in industrial applications where such packages cannot be avoided. Indeed, we only need to linearize the cost function dependency with respect to geometrical quantities over the shape (normals and surfacic triangles in 3D basicly). Hence, automatic differentiation or complex variable method become the best choices as usually this part of the code (i.e. CAD-Free definition, shape deformation, shape based geometrical quantities evaluation, cost function evaluation) is provided by the user and is application dependent.

6. Applications

Aeroelastic simulation were performed using CAD-Free structural models for two and three dimensional flows. The problem of interest is to predict aeroelastic behaviour of the coupled system and to control situations where the structure behaviour

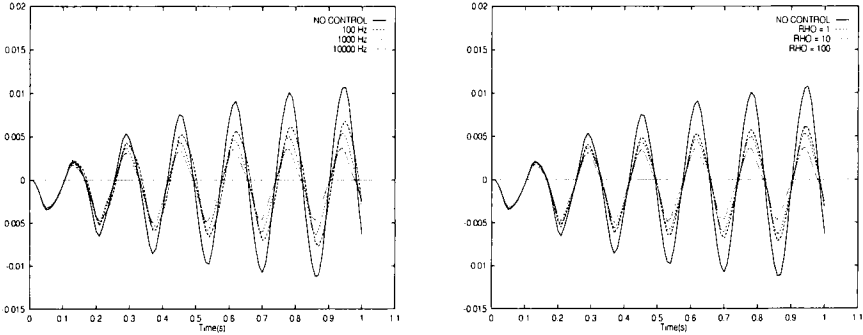


Figure 2. Control frequency (left) and descent amplitude ρ (right) impacts on control for a vertical inflow impact. Control conditions: $h = 10^{-6}$, $\rho = 1, 10, 100$, $f = 100\text{ Hz}, 1000\text{ Hz}, 10000\text{ Hz}$, maximum deviation $\alpha_{max} = +/ - 10\text{ degrees}$. The efficiency decreases with the frequency of control and its amount, for a given maximum deviation

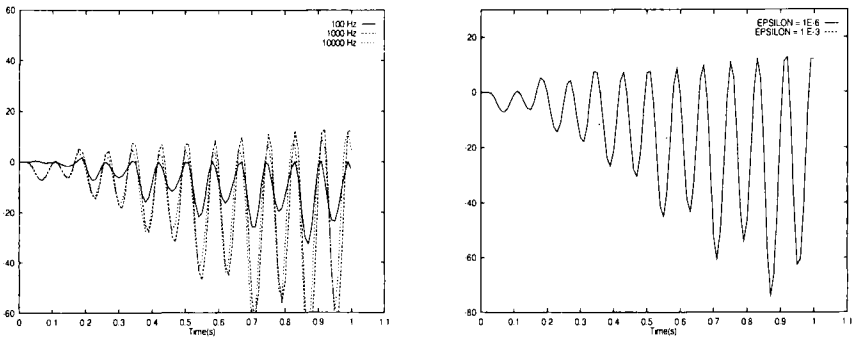


Figure 3. Control frequency (left) and h -increment (right) impacts on sensitivities for a vertical inflow impact. Control conditions: $h = 10^{-3}, 10^{-6}$, $\rho = 100$, $f = 100\text{ Hz}, 1000\text{ Hz}, 10000\text{ Hz}$, maximum deviation $\alpha_{max} = +/ - 10\text{ degrees}$

becomes unstable due to fluid perturbations. Control has been performed for all cases using flap deflection to change the flow (for the panel case) or the body incidence (for the wing and the aircraft cases). The flap deviation, as explained above, is prescribed using a real time sensitivity equation.

The first case concerns a 2D panel at Mach 1.2. The structural behaviour has been chosen for the coupled model to be unstable. Our aim is to control this instability by a flap introducing a deviation of the inflow. The CAD-Free parametrization here

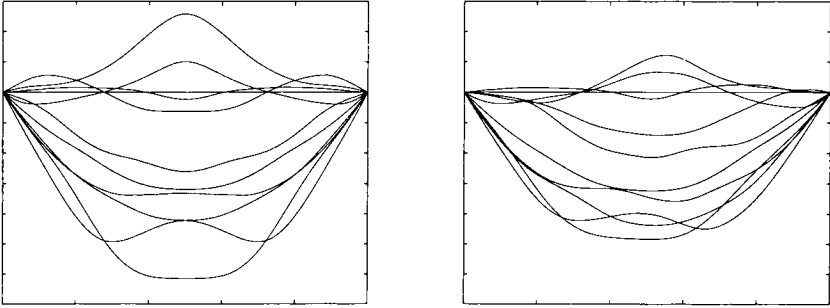


Figure 4. Snapshots of the membrane position without (left) and with (right) control for a zero incidence inflow. Control condition: $h = 10^{-6}$, $\rho = 100$, $f = 100\text{Hz}$, maximum deviation $\alpha_{max} = +/ - 10\text{degrees}$

has about 100 elements. The initial system has been perturbed by a displacement along the first panel eigenmode. We consider two cases corresponding to initial flows with zero and 90 degrees incidence. The former case represents therefore a vertical impact of the flow. We notice that for these cases the control is not enough efficient as it requires too much energy (maximum deviation angles required). In addition, the control efficiency increases with its update frequency which is not satisfactory from an industrial point of view, even if it makes sense. For these cases, a reasonable maximum deviation angle is about one or two degrees and an update frequency of a few Hertz (less than 10). Our control is therefore not enough efficient as it requires about 5-10 times more energy and update. This might be due to:

- imperfect numerics and coupling;
- the instantaneous control approach used instead of a global control. We recall that in the cost function (10), we removed the term $\int_0^T \alpha(t)^2 dt$ and only consider the following instantaneous cost function

$$\min_{\alpha(t)} J(\alpha(t)) = \int_{\partial\Omega(t)} (X(t) - X_{target})^2 d\gamma; \quad [14]$$

- the fact that only the steepest descent approach has been used which does not lead to the optimal control, but is only sub-optimal.

Surprisingly the situation is better for the 3D applications below.

The three dimensional cases concern flows over an M6 wing and a business Jet. The elastic CAD-Free parametrizations for these cases contain several thousands of elements and consists of surfacic triangular meshes. This surfacic mesh, as we said, is

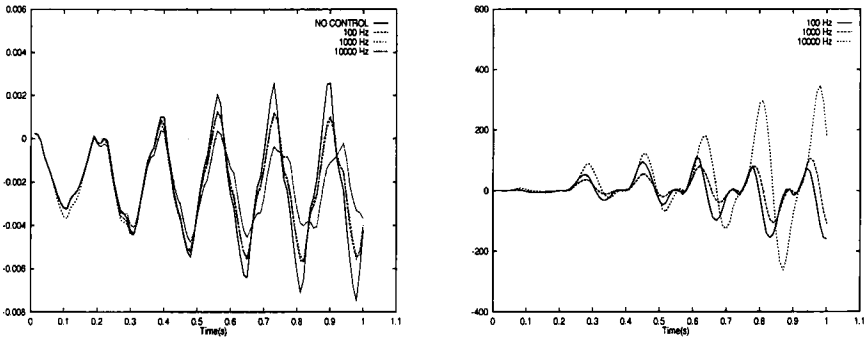


Figure 5. Control frequency impact on control (left) and sensitivities (right) for a zero incidence inflow. Control conditions: $h = 10^{-6}$, $\rho = 100$, $f = 100\text{ Hz}$, 1000 Hz , 10000 Hz , maximum deviation $\alpha_{max} = +/ - 10\text{ degrees}$

shared by fluid and structure codes in a more general coupling; something which really simplify the coupling strategies. In these cases, the fluid and structure system has been excited by an initial periodic incidence perturbation with frequency and amplitude (a few Hertz and degrees) corresponding to inflight observed situations:

the M6 case: $f \sim 2\text{ Hz}$, $-2 < \alpha_1 < 2$ degrees, $\alpha_2 = 0$ degrees,

the business jet case: $f \sim 10\text{ Hz}$, $-1 < \alpha_1 < 1$ degrees, $-1 < \alpha_2 < 1$ degrees,

where α_1 and α_2 are the two incidence angles for a 3D flow. These perturbations might happen in stormy weather or during take-off and landing in the wake of bigger aircrafts.

The same values have been used for the maximum incidences deviation during control. The control update frequency is twice the initial perturbation ones for each case. We show snapshots of shape deformation for each cases. The histories of the wing tips motion with and without the control applied show that this instantaneous control is quite efficient.

7. Conclusion

The application of the complex variable method to sensitivity analysis and definition of control laws for multi-model configurations has been presented. The approach seems to be quite insensitive to the choice of the increment for sensitivity analysis. This is interesting in multi-disciplinary applications. In addition, this enables a simultaneous evaluation of the functional and its sensitivity with respect to one control parameter. The physical problem concerns the control of 2 and 3D structures undergoing unstable structural behaviour due to flow perturbations. The dynamic control approach, based on instantaneous evaluation of sensitivities, gives only partly satis-

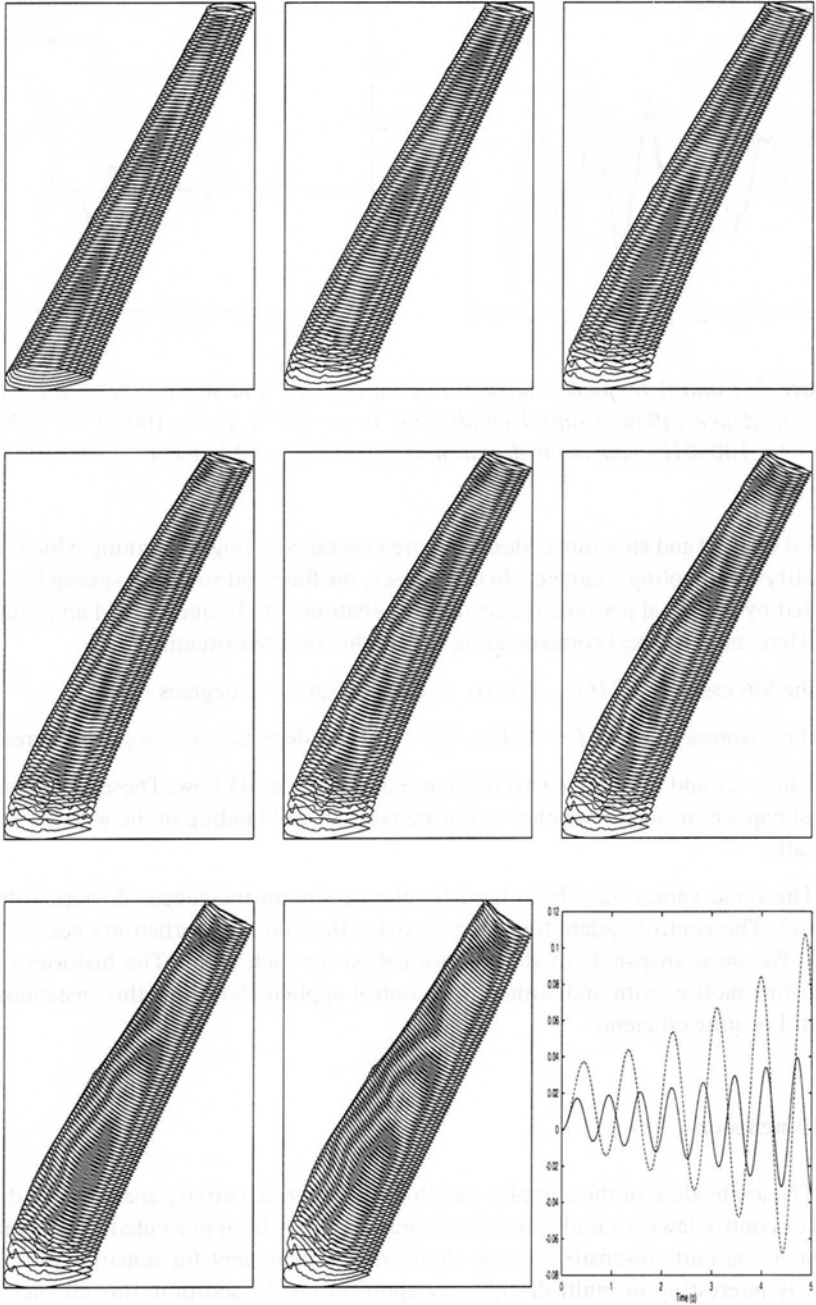


Figure 6. Aeroelastic simulation and control by stiffness identification for an M6 wing. Snapshots of the wing position without control. Last picture: wing tip vertical evolution

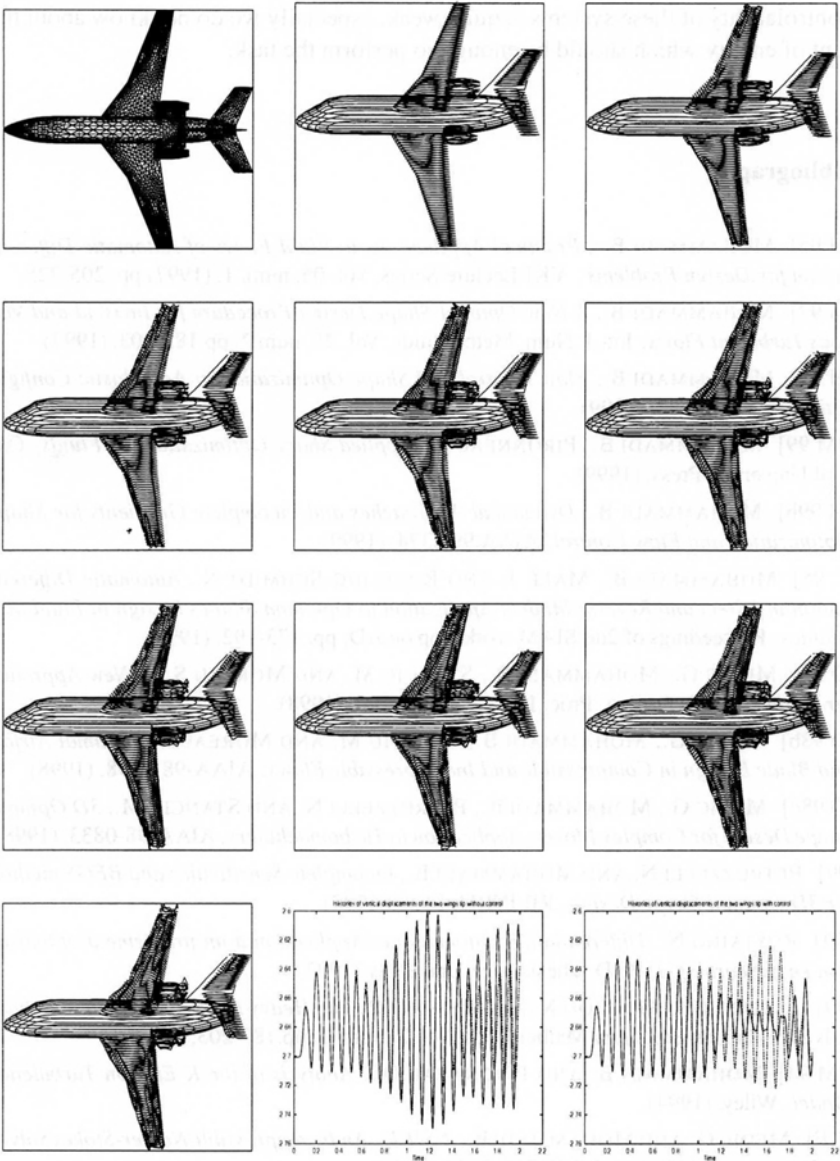


Figure 7. Aeroelastic simulation and control for a business jet. First picture: upper view of the CAD-Free parametrization. Snapshots of the shape without control. Last two pictures: left and right wing tips vertical evolutions without (left) and with control. The evolutions are not symmetric partly due to the fact that the CAD-Free parametrization is not

fraction as the required energy is still too high. However, our theoretical knowledge on the controlability of these systems is quite weak, especially we do not know about the amount of energy which should be enough to perform the task.

8. Bibliography

- [MOH 95] MOHAMMADI B., *Practical Applications to Fluid Flows of Automatic Differentiation for Design Problems*, VKI-Lecture Series, Vol. 05, num. 1, (1997) pp. 205-225.
- [MOH 97] MOHAMMADI B., *A New Optimal Shape Design Procedure for Inviscid and Viscous Turbulent Flows*, Int. J. Num. Meth. Fluids, Vol. 25, num.2, pp.183-203, (1997).
- [MOH 99] MOHAMMADI B., *Flow Control and Shape Optimization in Aeroelastic Configurations*, AIAA-0182, (1999).
- [OPBM 99] MOHAMMADI B., PIRONNEAU O., *Applied Shape Optimization for Fluids*, Oxford University Press, (1999).
- [MOH 99b] MOHAMMADI B., *Dynamical Approaches and Incomplete Gradients for Shape Optimization and Flow Control*, AIAA.99.3374, (1999).
- [MAL 95] MOHAMMADI B., MALÉ J. AND ROSTAING-SCHMIDT N., *Automatic Differentiation in Direct and Reverse Modes: Application to Optimum Shapes Design in Fluid Mechanics*, Proceedings of 2nd SIAM workshop on AD, pp. 173-192, (1995).
- [MED 98] MEDIC G., MOHAMMADI B., STANCIU M. AND MOREAU S., *A New Approach for Optimal Blade Design*, Proc. ICFD conf. Oxford, (1998).
- [MED 98b] MEDIC G., MOHAMMADI B., STANCIU M. AND MOREAU S., *Optimal Airfoil and Blade Design in Compressible and Incompressible Flows*, AIAA-98-2898, (1998).
- [MED 98c] MEDIC G., MOHAMMADI B., PETRUZZELLI N. AND STANCIU M., *3D Optimal Shape Design for Complex Flows: Application to Turbomachinery*, AIAA-98-0833, (1998).
- [PE 99] PETRUZZELLI N. AND MOHAMMADI B., *Incomplete Sensitivities and BFGS method for 3D Optimal Shape Design*, RR INRIA 3633, (1999).
- [RO 93] ROSTAING N., *Différentiation automatique: Application à un problème d'optimisation en météorologie*, Ph.D. Thesis Nice University (1993).
- [AT 99] ATTOUCH H., GOUDOU X. AND REDONT P., *The Heavy Ball with Friction Method*, Advances in Contemporary Mathematics, Vol. 2, num. 2, pp.183-203, (1999).
- [OPBM 94] MOHAMMADI B. AND PIRONNEAU O., *Analysis of the K-Epsilon Turbulence Model*, Wiley, (1994).
- [NSIKE] MEDIC G. AND MOHAMMADI B., *NSIKE - An Incompressible Navier-Stokes Solver for Unstructured Meshes*, RR INRIA 3644, (1999).
- [NSC2KE] MOHAMMADI B., *CFD with NSC2KE: an User Guide*, Technical INRIA report 164, (1994).
- [DO 92] DONEA J., *An ALE Finite Element Method for Transient Fluid-Structure Interactions*, Comp. Meth. App. Mech. Eng., Vol. 2, num. 33, pp. 689-723, (1982).
- [CA 96] FARHAT C. AND LESOINNE M., *On the Accuracy, Stability and Performance of the Solution of Three-dimensional Nonlinear Transient Aeroelastic Problems by Partitioned Procedures*, AIAA-96-1388, (1996).

- [NG 94] NKONGA B. AND GUILLARD H., *Godunoc Type Method on Non-Structured Meshes for Three Dimensional Moving Boundary-Problems*, Comp. Meth. App. Mech. Eng., Vol. 10, num. 113, pp. 183-204, (1994).
- [OP 84] PIRONNEAU O., *Optimal Shape Design for Elliptic Systems*, Springer, (1984).
- [SP 95] PIPERNO S., FARHAT C. AND LARROUTUROU B., *Partitioned Procedures for the Transient Solution of Coupled Aeroelastic Problems*, Comp. Meth. App. Mech. Eng., Vol. 11. num. 124, pp. 97-201, (1995).
- [ME 98d] MEDIC G., MOHAMMADI M. AND STANCIU M., *Prediction and Aeroelastic Simulation of Turbulent Flows in Civil Engineering Applications*, Proc. ECCOMAS 98, Athens (1998).
- [AN 98] ANDERSON K., NEWMAN J., WHITFIELD D. AND NIELSEN E., *Sensitivity Analysis for the Navier-Stokes Equations on Unstructured Grids Using Complex Variables*, AIAA-98-239, (1998).
- [SQ 98] SQUIRE W. AND TRAPP G., *Using Complex Variables to Estimate Derivatives of Real Functions*, Siam review, Vol. 10, num.1, pp.110-112, (1998).